Simulation and evaluation of a new PET system based on liquid xenon as detection medium

Jean-Pierre Cussonneau, C. Grignon, L. Luquin, Vincent Métivier, Noël Servagent

Simulation and evaluation of a new PET system based on liquid xenon as detection medium

J.P. Cussonneau[*], T. Carlier[1], O. Couturier[1], L. Ferrer[1], C. Grignon, L. Luquin, V. Métivier, F. Phéron, N. Servagent, D.Thers, A.Vasseur[1]

Subatech, Ecole des Mines de Nantes, IN2P3- CNRS and Université de Nantes, France
[1] Service de médecine nucléaire, Hôpital de Nantes, France

ABSTRACT: Due to its intrinsic physical properties, high density and atomic number, fast scintillation, high scintillation light yield and low ionization potential, liquid xenon is an excellent medium for the tracking and the accurate energy measurement of γ-rays in the MeV energy domain. The use of liquid xenon associated to a micro gap structure device to measure 511 keV γ-rays in PET tomograph is under investigation at Subatech. A GEANT3 simulation of a full PET design made of LXe-TPC modules has been developed and the first estimations of the performances from a realistic detector are very promising: good overall sensitivity to 511 keV γ-rays (~ 93% for a 9 cm depth LXe module), good three-dimensional spatial resolution (250 μm FWHM on the localization of the first interaction vertex). The measurement of the 3 coordinates of the interaction vertices and the energy loss associated allow to reconstruct the Compton sequence of correlated annihilation photons. Hence the capability to identify the first interaction vertex leads to major progresses in PET imaging: a parallax free PET tomograph with a high detection sensitivity of 190 kcps/kBq/ml and a 3-dimentionnal spatial resolution of 1.7 mm close to the physical intrinsic limits. The performances of the proposed LXe PET design are compared to a standard BGO PET camera operating in 3D acquisition mode.

1. INTRODUCTION

Simulations of a full liquid xenon based camera have been performed at Subatech to demonstrate the relevance of such a technique for PET applications. Compared to the commonly used crystals as for instance BGO or LSO, the liquid xenon detectors have the capability of localizing in 3 dimensions the interaction vertices of γ-rays with a resolution better than 1 mm and to accurately measure the associated energy loss. This 3 dimensional localization associated to the homogeneous response of LXe detectors can solve one of the main limitation of current PET camera performances i.e. the parallax error that occurs in crystal PET for γ-rays entering with oblique angles. For that purpose, a promising solution is to measure both the scintillation light and the ionization signal in a Liquid Xenon Time Projection Chamber LXe-TPC. The technical aspects of the proposed detector are discussed in reference[1].

2. SIMULATION OF A LXe-TPC PET

The simulation of a full PET camera was performed by using GEANT3 as Monte Carlo simulator, ROOT[2] as framework and AliRoot[3] as interface to the Monte Carlo. The parameterization of the low energy electron range in the liquid xenon was obtained separately from the dedicated Monte Carlo Casino[4]. The PET camera (Fig. 1) consists of 8 identical modules of $24\times60\times9\,cm^3$ fidutial volume settled according to a cylindrical geometry. Each module is subdivided in individual cells of $1\times1\times9\,cm^3$ volume delimited by PTFE walls to guide the scintillation light up to the VUV photo-detectors. To fully benefit from the good 3 dimensional spatial resolution and of the good energy resolution of the LXe-TPC modules, a large acceptance PET camera with a large axial field of view (60 cm) and a small diameter (60 cm) has been simulated and evaluated.

[*] Corresponding author, Phone: +33 2 51 85 84 31, E-mail: jean-pierre.cussonneau@subatech.in2p3.fr

Physical properties of liquid xenon and characteristics of the response of individual cells used as input parameters for the simulation are the following:

- The mean energy needed to create an electron/ion pair in LXe is taken to be W_i = 15.6 eV. 10% of the produced ionization electrons are subjected to the recombination for a 2 kV/cm drift electric field. The LXe purity is assumed to be perfect and then electrons are drifting along the 9 cm depth cell without any captures.
- An uncertainty on the drift time measurement of σ_t = 10 ns was considered and leads to a good spatial resolution of σ_z = 23 μm as the drift velocity is known to be 2.3 mm/μs for a 2 kV/cm electric field
- The transverse diffusion of the electrons moving toward the anode readout plane is taken to be 170 μm per root of centimeter of drift length[5].
- The $24\times60\,cm^2$ anode plane is segmented in $0.5\times0.5\,mm^2$ pads multiplexed in 48+60 strips utilizing a "checkerboard" readout scheme[1].
- The intrinsic energy resolution has been chosen to be $0.059\sqrt{E(MeV)}$ (FWHM)[6]. This can be seen as a conservative value but no additional deterioration due to the micro-mesh has been considered. For instance, the transparency of the micro-mesh to the electrons is supposed to be 100%.
- The electronic noise on each readout strip is assumed to be 300 e^- (RMS). Such a noise level can be reasonably reached with existing amplifiers. A zero suppression applied to the ionization signal on each readout channel leads to a 60 keV threshold on the energy deposited by electrons.
- the efficiency to detect VUV scintillation light with photo-detectors for electron of energy higher than ~50 keV is assumed to be 100 %.

The dependence of the energy resolution for 511 keV incident γ-rays with respect to the electron energy is shown in (Fig. 2); typically an energy resolution of ~5% is achieved for 511 keV electrons. The reconstructed energy of 511 keV γ-rays is then the sum of the single electron energies and shows a resolution of 13.8 % FWHM. The spatial resolution (Fig. 3) is dominated by the electronic noise at low energy for the x and y coordinates and by the electron range in liquid xenon at higher energy for the three coordinates. The accuracy on the localization of the first interaction vertex of 511 keV γ-rays in LXe which is of interest for the PET is found to be very satisfactory: 250, 250 and 140 μm (FWHM) for x, y and z coordinates respectively.

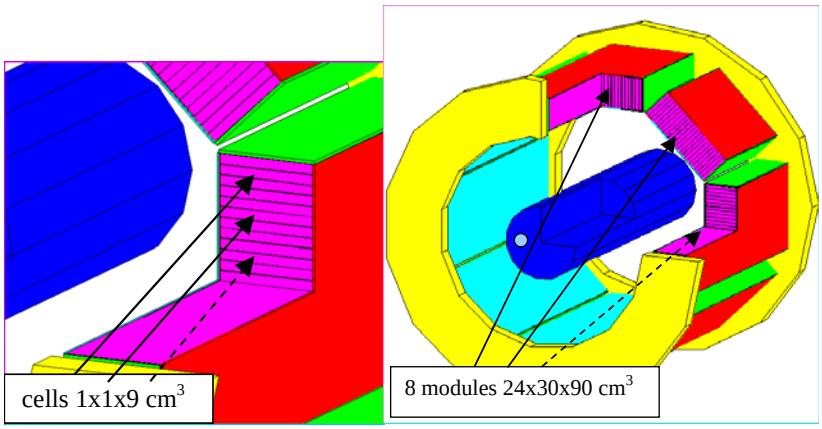

Fig. 1. GEANT3 simulation of a LXe PET camera with a NEMA NU 2-2001 phantom (right) and zoom on individual cells (left). The ^{18}F source is homogeneously distributed in a 3 mm diameter and 70 cm length cylinder positioned at (x=4.5 cm, y=0 cm) in the transverse field of view.

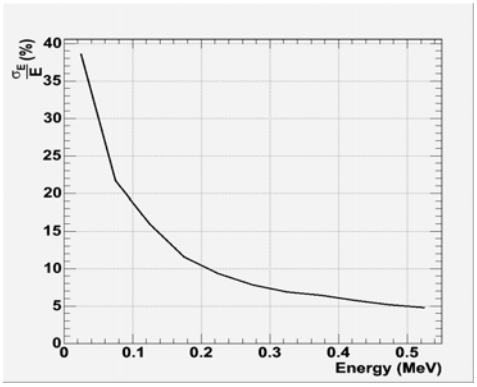

Fig. 2. Energy resolution as a function of the energy loss by electrons in LXe.

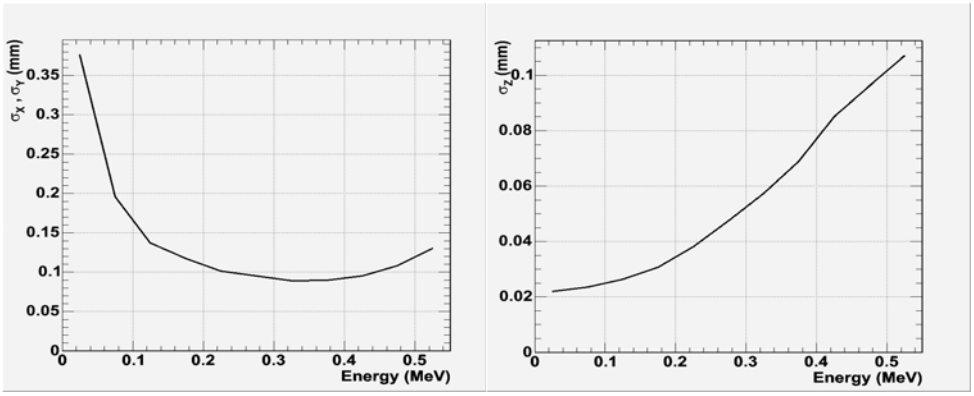

Fig. 3.Spatial resolution on the anode readout plane x,y (left) and spatial resolution from the drift time measurement z (right) as a function of the energy loss by electrons in LXe

3. RESULTS AND COMPARISON WITH A 3D BGO PET

A NEMA NU 2-2001 phantom[8] has been implemented in the simulation to evaluate the PET camera performances in 3D mode. The ^{18}F source is uniformly distributed in a 3 mm diameter and 70 cm length cylinder displaced at a radius of 4.5 cm from the camera center. The reconstruction of the line of response defined by the first interaction vertices of the two annihilation photons required a dedicated algorithm. This algorithm should be able to identify the first interaction vertex, especially in case of multiple Compton scattering of annihilation γ–rays in liquid xenon. Its main line is to build a χ^2 between the measured coordinates of the interaction vertices of the photons and the predicted ones calculated from the energy measurements and the theoretically known Compton kinematics. The Compton sequence reconstruction algorithm is similar to the method described in[7] , except that for PET the energy of the incoming annihilation γ-rays is constant.

The distribution of the closest distance of approach of the reconstructed line of response to the emission point is shown in (Fig. 4). A 3 mm cut off on this distance has been chosen to define the true and the scattered events leading to a fraction of 54.5% of the reconstructed lines considered as bad tracks. These reconstructed tracks with large distance of approach have two different origins, the first one is the scattering of photons in the water before entering in the liquid xenon (38%), the second one is the misidentification of the first interaction vertex by the Compton sequence reconstruction algorithm (16.5%).

The PET camera performances in terms of signal to noise ratio can be estimated by the construction of the noise equivalent count rate NEC :

$$NEC = \frac{T^2}{T + S + 2R}$$

Where, the true T and scattered S event rates was derived from the injected activity concentration C, the phantom volume V and the probability of reconstructing the line of response $p_{T,S}$ for the true and scattered events respectively:

$$\mathrm{T,S} = \mathrm{C} \times \mathrm{V} \times p_{T,S} \times (1 - Occ)^2$$

The number of hits per cell in the time window defined by the detector dead time τ=39.1 μs follows a binomial law and then the mean occupancy probability of one cell Occ is given by:

$$\mathrm{Occ} = 1 - (1 - p)^{C \times V \times \tau}$$

Where p the probability to fire one cell per event is coming from the simulation.

The mean random event rate (R) can be approximated by:

$$R = (C \times V \times p_{\sin} \times (1 - Occ))^2 \times \Delta t \times A$$

Where A is the azimuth acceptance of the PET depending on the phantom size, Δt = 10 ns is the time coincidence window and p_{sin} is the probability to have only one γ candidate per simulated event in the whole camera and in the energy window defined as (511±3×30 keV).

The NEC rate and its components are plotted separately against the activity concentration in (Fig. 5). The main performances are summarized in (table 1) and they are compared to the one of a standard BGO PET running in 3D acquisition mode. The BGO PET camera has been simulated with the same program and its main characteristics are a global size of 15 cm for the axial field of view and 80 cm for the diameter, the depth of the crystals is 30 mm and its transverse dimensions are 8×4 mm^2. The results of the simulation with a NEMA NU 2-2001 phantom are shown in (Fig. 5). The detector dead time resulting from the decay time of the BGO scintillation light has been set to 2.6 μs. No data acquisition dead time has been considered for both LXe and BGO cameras.

As it can be seen from (table 1) the proposed LXe PET camera can reach the NEC rate of 30 kHz that is a common value for standard whole-body BGO camera at 7.5 times lower activity concentration, with ~6 times higher sensitivity and a better spatial resolution.

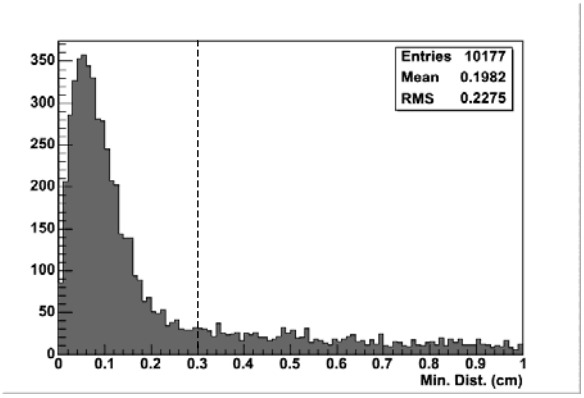

Fig. 4. Distribution of the closest distance of approach of the reconstructed line of response to the positron emission point. A 3 mm cut off on this distance has been chosen to discriminate between true and scattered events. The scatter fraction is then estimated to be 54.5 % from which the contribution of misidentified first interaction vertex is about 16.5 %.

PET camera	Activity (kBq/ml)	Sensitivity – Net Trues (cps/Bq/ml)	Spatial cut (spatial resolution FWHM) (mm)	Energy resolution (FWHM)
BGO	3	30	10 (~7)	26.7
LXe	0.4	190	3 (~1.7)	13.8

Table 1: Performances of the proposed LXe-TPC PET compared to a standard BGO PET camera.

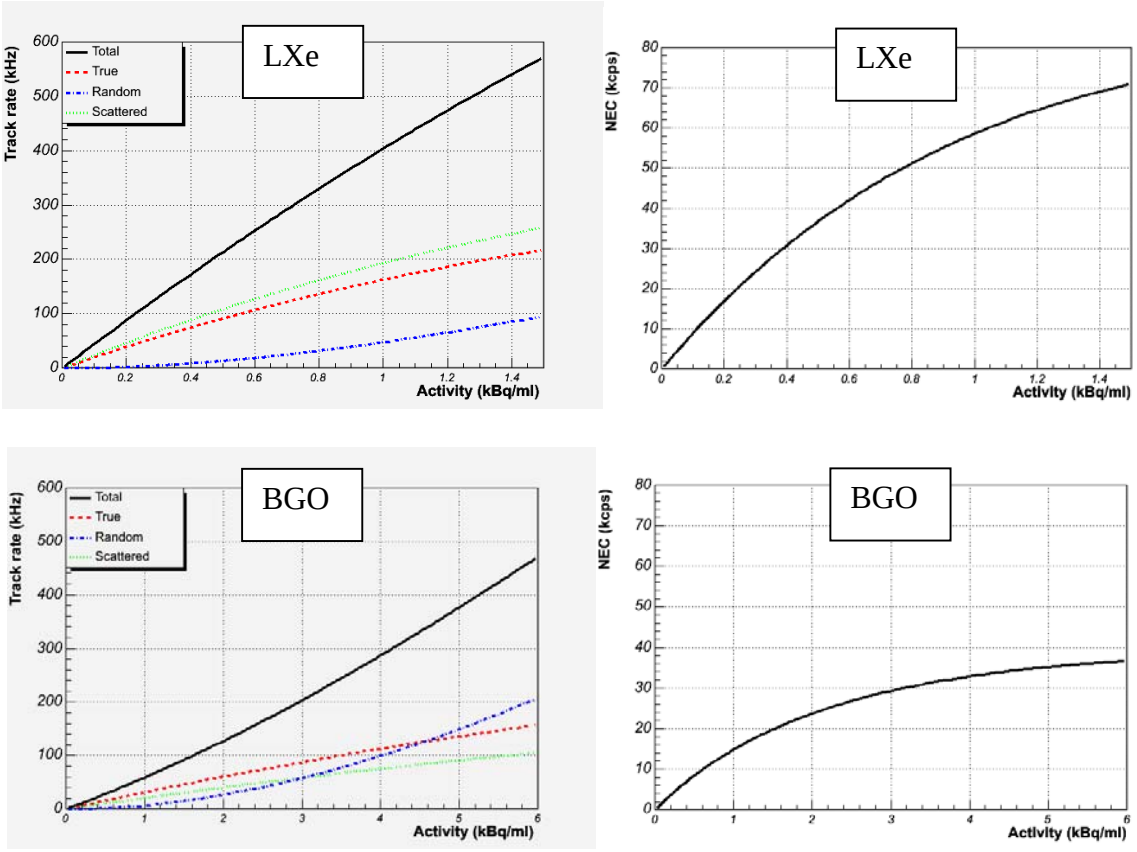

Fig. 5. Track rate for true, scattered and random events (left) and NEC (right) as a function of the activity concentration for the proposed LXe-TPC PET (top) and the standard BGO camera (bottom).

4. CONCLUSIONS

In conclusion, the proposed LXe-TPC PET shows good overall performances for whole-body imaging. Its performances were evaluated with a NEMA NU 2-2001 phantom and compared to those of a BGO PET camera. To fully benefit from the 3D localization of LXe-TPC, a large acceptance tomograph (60 cm in axial FOV and 60 cm in diameter) has been envisaged. The camera sensitivity is then increased without deterioration of the spatial resolution as it is parallax free. Moreover the expected energy resolution is good enough to limit the increase of the scattered fraction because of the larger phantom thickness seen by the γ-rays. Although the detector dead time is larger for a LXe-TPC than for a crystal PET camera, the large acceptance allows to reach the same NEC rate at a lower activity concentration.

REFERENCES

[1] D. Thers et al. XeSAT2005 proceedings
[2] Root, http://root.cern.ch
[3] AliRoot, http://AliSoft.cern.ch/offline.
[4] Casino, http://www.gel.usherb.ca/casino
[5] T. Doke & al., T.Ferbel book
[6] E. Aprile et al., Nucl. Inst. Meth. A480 (2002) 636-650
[7] E. Aprile et al., arXiv:astro-ph/0212005 v2 4 Dec 2002.
[8] NEMA Standards Publication NU 2-2001, Nationnal Electrical Manufacturers Association.